SCIENCE CHINA Chemistry

Molecular engineering tuning optoelectronic properties of thieno[3,2-b]thiophenes-based electrochromic polymers

Zhu Mengmeng, Li Weishuo, Xu Panpan, Shi Jingjing, Shao Shan, Zhu Xiaosi, Guo Yitong, He Yaowu, Hu Zhao, Yu Hongtao, Zhu Yanan, Perepichka Igor F. and Meng Hong

Citation: SCIENCE CHINA Chemistry **60**, 63 (2017); doi: 10.1007/s11426-016-0305-9

View online: http://engine.scichina.com/doi/10.1007/s11426-016-0305-9

View Table of Contents:http://engine.scichina.com/publisher/scp/journal/SCC/60/1

Published by the Science China Press

SCIENCE CHINA Chemistry

SCIENCE CHINA
Chemistry

• FEATURE ARTICLES •
• SPECIAL TOPIC • Electrochromics

January 2017 Vol.60 No.1: 63–76
doi: 10.1007/s11426-016-0305-9

Molecular engineering tuning optoelectronic properties of thieno[3,2-*b*]thiophenes-based electrochromic polymers

Mengmeng Zhu[1], Weishuo Li[1], Panpan Xu[1], Jingjing Shi[1], Shan Shao[1], Xiaosi Zhu[1], Yitong Guo[1], Yaowu He[1], Zhao Hu[1], Hongtao Yu[1], Yanan Zhu[1], Igor F. Perepichka[2] & Hong Meng[1*]

[1]*School of Advanced Materials, Peking University Shenzhen Graduate School, Shenzhen 518055, China*
[2]*School of Chemistry, Bangor University, Bangor LL57 2UW, United Kingdom*

Received July 18, 2016; accepted September 27, 2016; published online December 7, 2016

Thieno[3,2-*b*]thiophene (TT) monomers end-capped with 3,4-ethylenedioxythiophene (EDOT) moieties are electropolymerized to form π-conjugated polymers with distinct electrochromic (EC) properties. Steric and electronic factors (electron donor and acceptor substituents) in the side groups of the TT core, as well as the structure of the polymer backbone strongly affect the electrochemical and optical properties of the polymers and their electrochromic characteristics. The studied polymers show low oxidation potentials, tunable from –0.78 to +0.30 V (vs. Fc/Fc^+) and the band gaps from 1.46 to 1.92 eV and demonstrate wide variety of color palettes in polymer films in different states, finely tunable by structural variations in the polymer backbone and the side chains. EC materials of different colors in their doped/dedoped states have been developed (violet, deep blue, light blue, green, brown, purple-red, pinkish-red, orange-red, light gray, cyan and colorless transparent). High optical contrast (up to 79%), short response time (0.57–0.80 s), good cycling stability (up to 91% at 2000 cycles) and high coloration efficiency (up to 234.6 cm^2 C^{-1}) have been demonstrated and the influence of different factors on the above parameters of EC polymers have been discussed.

electrochromic, conducting polymer, electrochemistry, thieno[3,2-*b*]thiophene, EDOT

Citation: Zhu M, Li W, Xu P, Shi J, Shao S, Zhu X, Guo Y, He Y, Hu Z, Yu H, Zhu Y, Perepichka IF, Meng H. Molecular engineering tuning optoelectronic properties of thieno[3,2-*b*]thiophenes-based electrochromic polymers. *Sci China Chem*, 2017, 60: 63–76, doi: 10.1007/s11426-016-0305-9

1 Introduction

Electrochromism is the phenomenon of reversible optical change in a material induced by an external voltage which results in its electrochemical oxidation or reduction producing the states of distinctly different electron absorption spectra [1]. The concept of "electrochromism" was first theoretically proposed by Platt in 1961 [2].

Since the first demonstration of an electrochromic (EC) effect, numerous EC materials have been developed and they have found a wide range of applications [3], such as "smart windows/mirrors" [4,5], automatic anti-glazing mirrors [6], sunglasses [7], electronic paper [8], display panels [9], data storage [10], electrochromic textile/fabric devices [11,12], spacecraft and military applications [13,14].

Polymeric EC materials with incorporated electro/photoactive chromophores into the main chain of non-conjugated polymers have been recently reviewed by Liaw *et al*. [15].

Conjugated polymers (CPs) have attracted tremendous interest in the past decades due to their unique properties and wider range of possible applications, which were highlighted in many nice reviews [16,17]. Variety of structural variations and modifications of the backbone and the side chains

*Corresponding author (email: menghong@pkusz.edu.cn)

in EC conjugated polymers, potentially low cost production and possibility for large-area flexible device fabrication, high coloration efficiency and extreme chromatic diversity, fast response time, excellent redox and environmental stability and good optical memory, all these make them invaluable EC materials for many technological applications with great potential for commercialization. The color hue and the band gap in CPs EC materials can be relatively easily and precisely tuned by structural modification of used monomers to match with the application needs. Many efforts have been made in the past two decades to expand the "color palette" of CPs EC materials by incorporation of various building blocks into the main polymer chain, to tune the electronic energy levels in the reduced/oxidized states of CPs and their band gaps, to control the sterics (e.g. to adjust the planarity of the polymer backbone), as well as to improve the stability of the materials and devices [18–20].

In the end of 1980s, chemists at the Bayer AG company put forward a novel conducting polymer poly(3,4-ethylenedioxythiophene) (PEDOT) [21], which made remarkable progress in the field. PEDOT has low band gap of ca. 1.6 eV (in an undoped state), low oxidation potential, tremendous stability, and high conductivity and optical transparency in its doped state [22–26]. It was commercialized under the trademark Baytron® (then as Clevios™) and is now widely used as electrically conductive and hole injection layer (in the doped form, PEDOT:PSS, with polystyrene sulfonate) in various electronic applications including organic antistatic coatings, light emitting diodes (OLED), organic photovoltaic cells (OPV), as well as in EC devices [27,28]. Considering the unique properties of PEDOT, a lot of research has been done on functionalization of its monomer 3,4-ethylenedioxythiophene, EDOT (Scheme 1), at the side ethylene bridge (as well as on its ring-expanded analog 3,4-propylenedioxythiophene, ProDOT, Scheme 1), with numerous reports on synthesis and studies of a wide range of novel polymers and copolymers based on these building blocks [29–32].

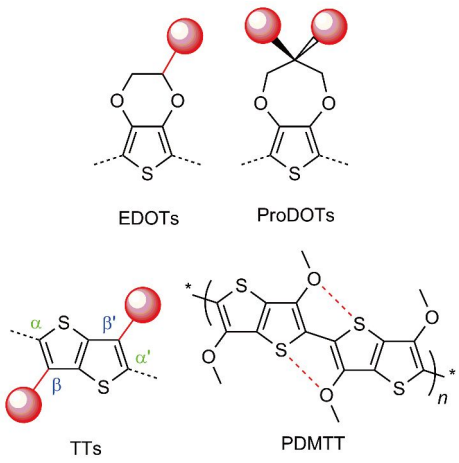

Scheme 1 Structures of EDOTs, ProDOTs, TTs and PDMTT (color online).

Thieno[3,2-*b*]thiophene (TT) (Scheme 1) [33,34] represents another popular fused thiophene building block, which is now widely used in design of novel polymeric materials for OPV [35], OLED [36,37], OTFT (organic thin film transistors) [38] and EC materials [39]. With its rigid and planar structure, extended conjugation and easy functionalizations at β,β′ (3,6-) positions, TT offers many opportunities in the design of novel high performing electronic materials. Thus, in 2005 Roncali group [40] has reported a novel low band gap (E_g=1.65 eV) polymer based on 3,6-dimethoxythieno[3,2-*b*]thiophene (DMTT), PDMTT (Scheme 1), which has planar rigid structure due to short S··· O intramolecular contacts (similar to that existing in EDOT oligomers and PEDOT) and showed low oxidation potential, good stability, and optical transparency in the doped state (pale blue in the reduced state, λ_{max}=592 nm) comparable to that for PEDOT. Structural variations in β,β′ substituents can drastically change the optical properties and electrochromic behavior of TT-based polymers: bulky aryl groups in poly(3-arylthieno[3,2-*b*]thiophenes) give the polymers, which are reddish yellow to brown in their reduced state and blue in the oxidized state [41]. These examples demonstrate that thieno[3,2-*b*]thiophene core represents tremendous potential for constructing EC materials, including additional potential for α,α′/β,β′ cross-conjugation and cross-linked polymers.

Consequently, combination of TT and EDOT building blocks in the construction of novel electrochromic polymers can offer wide range of opportunities to control the optical and electrochemical properties of materials, their stability, coloration efficiency and other important characteristics of EC materials and devices.

2 Design principle and synthesis of EDOT-TT-EDOT electrochromic materials

Here, we highlight recent research on the design and systematic studies of a series of materials based on EDOT-TT-EDOT core to demonstrate conceptual design of novel EC polymers and to show the relationships between the structural effects of different donor and acceptor substituents in the β,β′-positions of TT units and the optoelectronic properties of electrogenerated polymers from such materials. The principle is depicted in Chart 1: planar backbone along EDOT-TT-EDOT gives the polymers with low oxidation potential and narrow band gap, whereas functionalization with R side groups allows fine tuning the electronic and optical properties of polymers in the dedoped/doped state by proper choice of substituents, as well as an additional opportunity for an expansion of conjugation into the second dimension toward cross-conjugated materials. In this study, benzene, thiophene

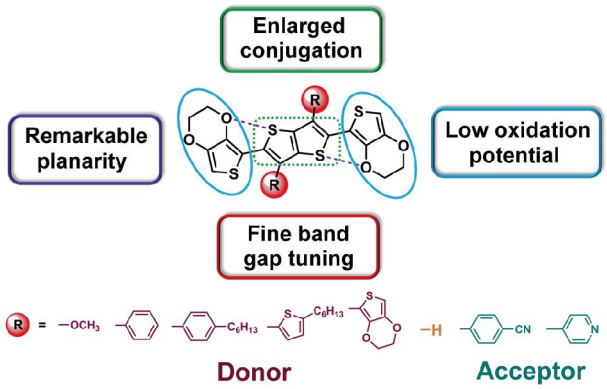

Chart 1 Schematic representation of the design of EC materials based on thieno[3,2-*b*]thiophene (TT) core (color online).

and EDOT are chosen as donor while pyridine and cyano units as acceptor substituents. In addition, *n*-hexyl is introduced to further study the influence of the insulating character and the intermolecular interaction resulted from aliphatic chain. We focus on analysis of tuning the optical and electrochromic properties of CPs by judicious choice of the substituents and fashion of conjugation in the EDOT-TT-EDOT core.

The general synthetic route employed by our group [42–44] recently to access monomers **M1**–**M8** is shown in Scheme 2. It is based on consecutive functionalization of thieno[3,2-*b*]thiophene core at positions 3,6-(**1**→**2,3**) and then 2,5-(**2,3**→**4**→**M1**–**M8**). Scheme 3 also shows two other isomeric monomers **M9** and **M10** used for comparative studies of the positional effect of EDOT-TT-EDOT core on EC properties of polymers [44].

3 Structural effects of EDOT-TT-EDOT monomers on their properties

3.1 Electron absorption spectra of monomers

The UV-Vis electron absorption spectra of monomers **M1**–**M10** are shown in Figure 1 and the data are summarized in Table 1. Unsubstituted monomer **M6** shows the longest wavelength absorptions (λ_{max}=390and 408 nm, with a shoulder at 455 nm) and fine vibronic structure of its absorption spectrum confirming the rigidity of the system. Similar long-wavelength, vibronically resolved absorptions are also observed for monomers **M1** and **M5** with methoxy and EDOT groups, respectively, at positions 3,6- in which cases intramolecular attractive S··· O interactions facilitate the planarization of the molecules [31,45–47]. Slight bathochromic shift λ_{max} from 408 nm (**M6**) to 413 nm (**M1**) due to introduction of electron-donating (and facilitating intramolecular S··· O interactions) methoxy group is in excellent agreement with studies on similar EDOT-TT-EDOT molecules with hexyl-end-capped EDOT fragments [48]. An incorporation

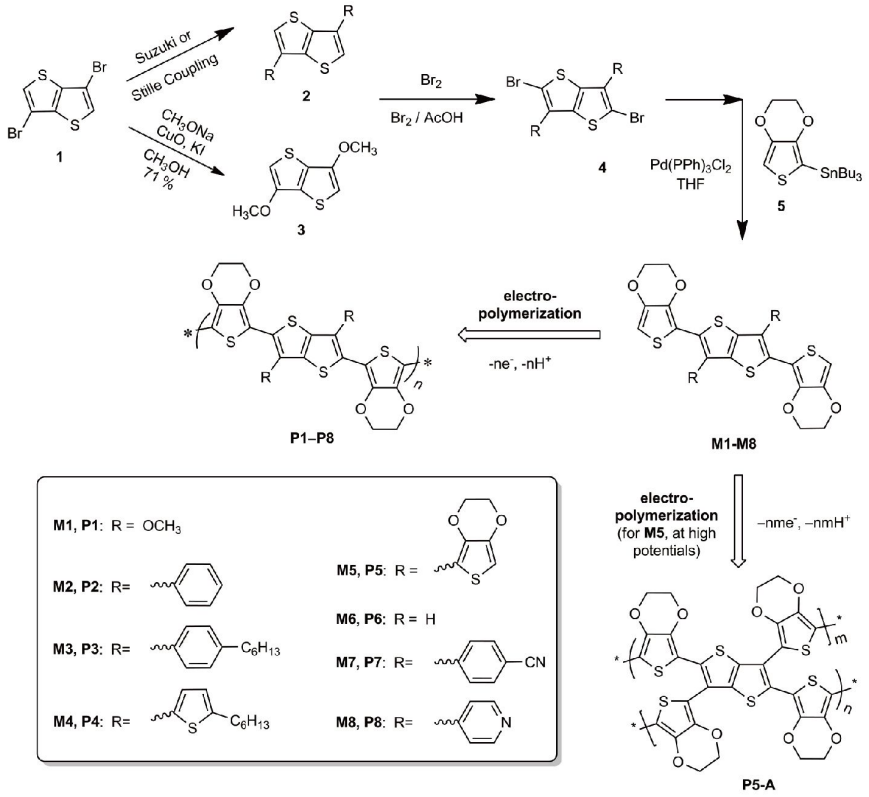

Scheme 2 The synthetic route to the monomers **M1**–**M8**, and their electropolymerization to polymers **P1**–**P8** and **P5-A** [42–44].

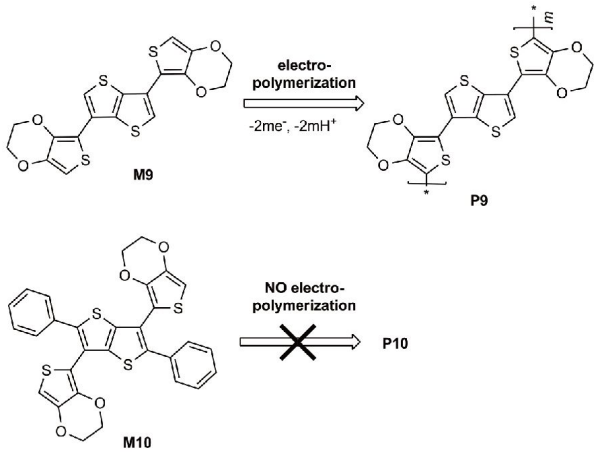

Scheme 3 Structures of monomers **M9** and **M10**, and electropolymerization of **M9** to **P9** [44].

of bulky aryl groups at positions 3,6-(**M2**, **M3**, **M4**, **M7** and **M8**) sterically perturb the conjugation along the EDOT-TT-EDOT and the planarity of the molecules, resulting in hypsochromic shifts of an absorption (down to λ_{max}=365–380nm) and in disappearance of vibronic structure in their electronic spectra. However, changes in the absorption spectra for 3,6-arysubstituted monomers are small and there is no clear correlations between their absorption maxima and the electron donating/accepting character of the substituents. It is worth noting that monomer **M4** with thiophene substituents at positions 3,6- shows hypsochromic shift compared to somewhat more bulky 3,6-EDOT-substituted analog **M5**, suggesting an important role of ethylenedioxy groups for narrowing the highest occupied molecular orbital (HOMO)-lowest unoccupied molecular orbital (LUMO) gap (with possible contribution from short S···O contacts to this difference, apart from stronger electron donating effect of EDOT). At the same time, drastic effect of the position of substitution (3,6- vs. 2,5-) on the degree of conjugation can be clearly seen when comparing the monomers **M9** with **M6** and **M10** with **M2**: shorter conjugation path and an increased steric hindrance for π-electron delocalization along the 3,6-positions in TT result in drastic hypsochromic shifts of the monomers absorptions (by ~70 and ~40 nm, respectively). Such an interpretation is in good agreement with B3LYP/6-31G(d) DFT calculations: while monomer **M6** is near planar (dihedral angles between the TT and EDOTs are ca. 1.5°), the monomer **M9** is substantially distorted (dihedral angles between the TT and EDOTs are ca. 51°).

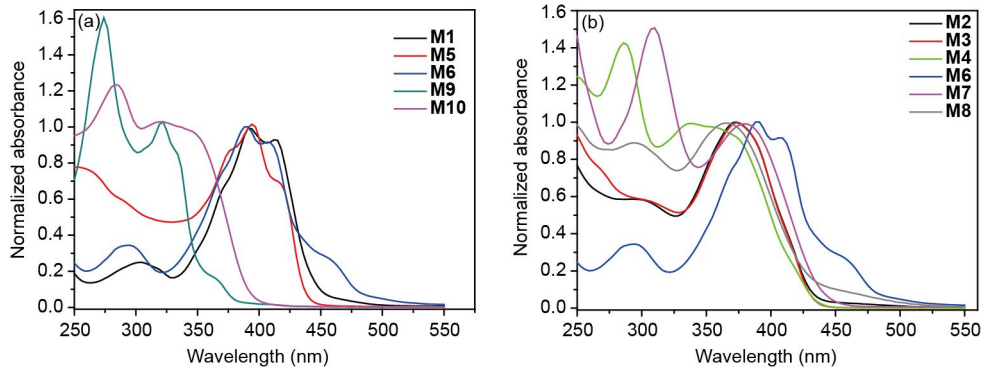

Figure 1 Electron absorption spectra of monomers **M1**–**M10** in $CHCl_3$ (the spectra are normalized to the longest absorption maxima) (color online).

Table 1 Electrochemical and optical data for thieno[3,2-*b*]thiophenes-based monomers **M1**–**M10**

Monomer	3,6-subst.	2,5-subst.	λ_{max}^{abs} (nm), [$CHCl_3$]	λ_{onset} a) (nm)	$E_{g,opt}$ a) (eV)	$E_{ox,onset}$ b) (V)	HOMO c) (eV)	LUMO d) (eV)
M1	MeO	EDOT	303, 372sh e), 393, 413	454	2.73	–0.05	–4.75	–2.02
M2	Ph	EDOT	374	438	2.83	0.10	–4.90	–2.07
M3	HexPh	EDOT	374	434	2.86	0.13	–4.93	–2.07
M4	HexTh	EDOT	286, 338	438	2.83	0.27	–5.07	–2.24
M5	EDOT	EDOT	355sh, 370sh, 378sh, 393, 415sh	438	2.83	0.06	–4.86	–2.03
M6	H	EDOT	293, 390, 408, 455sh	492	2.52	0.12	–4.92	–2.40
M7	CNPh	EDOT	309, 380	444	2.79	0.39	–5.19	–2.40
M8	Py	EDOT	294, 365, 450sh	447	2.77	0.34	–5.14	–2.37
M9	EDOT	H	273, 320	382	3.25	0.26	–5.06	–1.81
M10	EDOT	Ph	284, 321, 345sh	393	3.16	0.59	–5.39	–2.23

a) $E_{g,opt}$ is the HOMO-LUMO gap of the monomers, estimated from the red edge of their electron absorption spectra (λ_{onset}): $E_{g,opt}$=1240/λ_{onset} (eV); b) $E_{ox,onset}$ is the onset of electrochemical oxidation potentials (vs. Fc/Fc^+) of the monomers in dichloromethane/acetonitrile (DCM/ACN), 4:1 (**M1**), 3:1 (**M2, M3**), DCM (**M4**–**M6**, **M9**, **M10**), $CHCl_3$/ACN, 4:1 (**M7**), DCM/THF (THF=tetrahydrofuran), 3:2 (**M8**), 0.1 M tetrabutylammonium hexafluorophosphate ($TBAPF_6$), Pt working electrode, scan rate 100 mV s^{-1}; c) HOMO=–($E_{ox,onset}$+4.8)(eV); d) LUMO=HOMO+$E_{g,opt}$ (eV); e) sh: shoulder.

3.2 Electrochemical properties of the monomers

All the monomers are anodically oxidized showing irreversible oxidation waves with $E_{ox,onset}$ in the region of –0.05 to +0.59 V vs. Fc/Fc^+ (Figure 2 and Table 1). Compared to unsubstituted monomer **M6** ($E_{ox,onset}$=0.12 V vs. Fc/Fc^+), an introduction of electron donating EDOT groups (**M5**) and especially methoxy groups (**M1**) at positions 3,6- (which increases the HOMO energy level of the monomers) results in cathodic shifts of their oxidation potentials and **M1** shows the lowest oxidation potential in the series ($E_{ox,onset}$=–0.05 V). On the other hand, sterically hindered aryl groups (**M2** and **M3**) have very small effect on the oxidation potentials of the monomers (i.e. on HOMO), in contrast to their more pronounced effect on the absorption spectra (i.e. on HOMO-LUMO gap). The importance of electronic effect of substitutents in positions 3,6- is also seen from the comparison of **M6** with **M7** and **M8**, which shows anodic shifts of their oxidations by 0.22–0.27 V (to 0.39 and 0.34 V, respectively).

Anodic shift in the thiophene-substituted monomer **M4** compared to the phenyl analogs (**M2** and **M3**) by 0.14–0.17 V is somewhat unexpected considering the electron rich character of the thiophenes moiety. Possibly, it can be rationalized from the consideration of the geometries of 3.6- phenyl- and thienyl-substituted EDOT-TT-EDOT monomers, i.e. **M2**/**M3** vs. **M4**. Thus, DFT calculations show that dihedral angles between the TT core and side thienyl substituent (**M4**) is substantially higher (72°) than that for phenyls in **M2**/**M3** (49°) (Figure 3) decreasing the electron donating effect of the thiophenes moieties on the EDOT-TT-EDOT π-system by the resonance. Dihedral angles between TT and EDOT moieties are 39° and 7°, respectively. Similarly to the electron absorption spectroscopy data, the mode of location of EDOT units on the TT moiety (3,6- vs. 2,5-) has pronounced effect on their electrochemical behavior. Monomer **M9** (3,6-EDOT substitution) is more difficult to oxidize than **M6** (2,5-EDOT substitution) (by 0.14 V), and even more pronounced positive shift in oxidation by 0.49 V is observed for their phenyl-substituted analogs (**M2**→**M10**).

4 EDOT-TT-EDOT based electrochromic polymers

4.1 Electrochemical polymerization of the monomers

Monomers **M1**–**M9** are easily electropolymerized in potentiodynamic conditions with anodic scans to the potentials of their oxidations to the radical cations, with growing the polymer films on the surface of working electrode in cyclic voltammetry (CV) experiments, which is manifested by an appearance of increased waves at lower potentials on cycling (as exemplified in Figure 4 for electropolymerization of **M1** and **M6**). While the monomer **M9** with 3,6-attached EDOT groups can be electropolymerized (but at higher potentials than its 2,5-isomer **M6**), sterically crowded analog **M10** with bulky phenyl groups at positions 2,5- does not give corresponding polymer by electropolymerization process, in contrast to its isomer **M2** (Figure 2).

Monomer **M5** represents a special case, as it contains EDOT end groups attached to both 2,5- and 3,6-positions, which are oxidized at different potentials, with lower oxidation potentials for 2,5-EDOT substituted isomers compared to their 3,6-counterparts (compare **M6** vs. **M9** and **M2** vs. **M10**, Table 2). Accordingly, an electropolymerization can be potentially performed rather selectively and proper choice of an electropolymerization potential could give different type of polymers. Really, at lower electropolymerization potentials, the coupling occurs only at one type of EDOT groups (i.e. 2,5-) giving the linear polymer **P5** whereas at higher potentials, EDOT end groups on both sites (2,5- and 3,6-) are involved in the process resulting in cross-linked polymer **P5-A** (Scheme 2), properties of which differ substantially from **P5** (discussed below) [42].

4.2 Electrochemical properties of polymers P1–P9, P5-A and P11

The previous studies have demonstrated that there is little difference in the optoelectrochemical behaviors of polymers synthesized by chemical and electrochemical methods

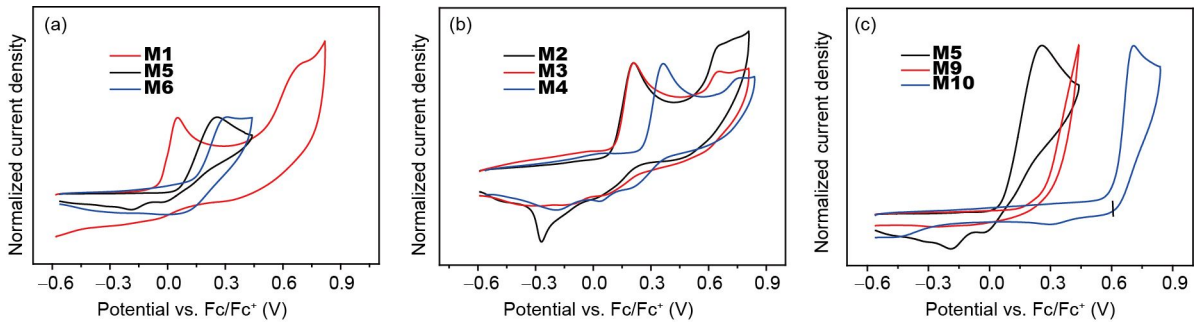

Figure 2 Cyclic voltammograms of monomers **M1**–**M6**, **M9** and **M10** on a Pt disk electrode at a scan rate 100 mV s^{-1}. Electrolyte is 0.1 M $TBAPF_6$, solvents are indicated in the Table 1 (color online).

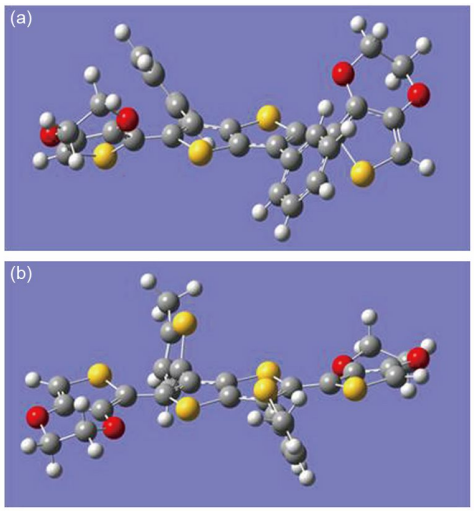

Figure 3 DFT B3LYP/G-31G(d) optimized geometries for (a) **M2** and (b) **M4** (hexyl group is substituted by methyl group for clarity of representation) (color online).

[49,50]. Apart from a series of electrochemically prepared polymers **P1**–**P9** and **P5-A**, chemically prepared soluble donor-acceptor polymer **P11** (Scheme 4) have been included for comparative considerations in this section. **M1**–**M9** are electron rich units (with some electron deficient character of the sidegroups in **M7** and **M8**) and it is worth to compare the electrochemical, optical and EC properties of the polymers prepared from these building blocks with related copolymer **P11** incorporating into its backbone the benzothiazole electron acceptor unit, which is successfully and widely used in donor/acceptor (D-A) copolymers for electrochromics [51], OPV [52], OLED [53] and OFET [54].

All the polymers show an electroactivity with the reversible p-doping/dedoping process. The CV traces of representative polymers are shown in Figure 5 and all the data are collated in Table 2. Scan rate dependent CV experiments (from 25 to 200 mV s^{-1}) for all the polymer films shows excellent linear dependences (correlation coefficients R^2=0.997–1.000)of the current densities versus the scan rates, for both anodic and cathodic currents, j_{pa} and j_{pc}, as exemplified in Figure 6 for **P1** and **P11**. This confirms that p-doping/dedoping process of the polymers is highly reversible and proceeds in non-diffusion conditions.

Oxidation (p-doping) of the polymer **P1** with electron donating methoxy groups (which also planarize the backbone

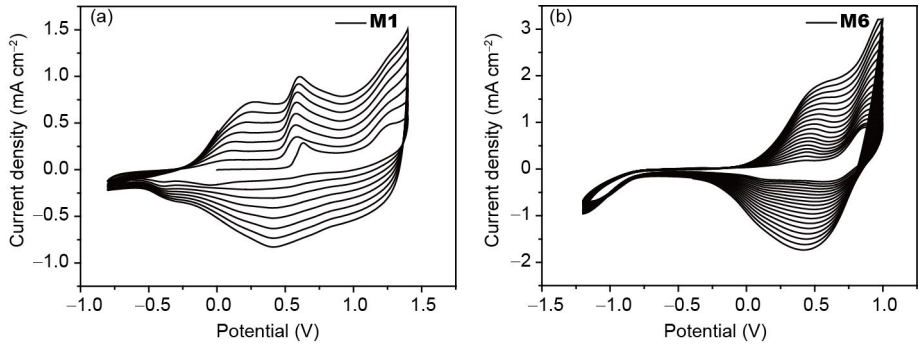

Figure 4 Electropolymerization of monomers **M1** and **M6** [44] on a Pt working electrode in DCM/ACN, 4:1 (**M1**) and DCM (**M6**) with 0.1 M $TBAPF_6$, on cycling at a scan rate 100 mV s^{-1}. Potentials are vs. Ag wire.

Table 2 Electrochemical and optical data for polymers **P1**–**P9**, **P5-A** and **P11** in films

Polymer	3,6-subst.	2,5-subst.	λ_{max}^{abs} a) (nm)	λ_{onset} a) (nm)	$E_{g,opt}$ b) (eV)	$E_{ox,onset}$ c) (V)	HOMO d) (eV)	LUMO d) (eV)	$\Delta E_{ox}^{M\text{-}P}$ e) (V)
P1	MeO	EDOT	579	822	1.51	–0.78	–4.02	–2.51	0.73
P2	Ph	EDOT	584, 638	689	1.80	–0.45	–4.35	–2.55	0.55
P3	HexPh	EDOT	596, 642	697	1.78	–0.42	–4.38	–2.60	0.55
P4	HexTh	EDOT	548	730	1.70	–0.37	–4.43	–2.73	0.64
P5	EDOT	EDOT	583	718	1.73	–0.53	–4.27	–2.54	0.59
P5-A	EDOT	EDOT	514	698	1.78	–0.26	–4.56	–2.78	0.36
P6	H	EDOT	569	721	1.72	–0.64	–4.16	–2.44	0.76
P7	CNPh	EDOT	580	808	1.53	–0.36	–4.44	–2.91	0.75
P8	Py	EDOT	545	745	1.66	+0.30	–5.10	–3.44	0.09
P9	EDOT	H	475	647	1.92	–0.25	–4.55	–2.63	0.51
P11	–	–	451, 683	852	1.46	–0.06	–4.74	–3.28	–

a) Absorption maxima and absorption onsets of the polymers in the dedoped state; b) optical band gaps of the neutral polymers; c) for the films on indium tin oxide (ITO) in monomer-free 0.1 M $TBAPF_6$/ACN vs. Fc/Fc^+; d) HOMO and LUMO energies are calculated similar to Table 1; e) differences between the $E_{ox,onset}$ for the monomers and the polymers.

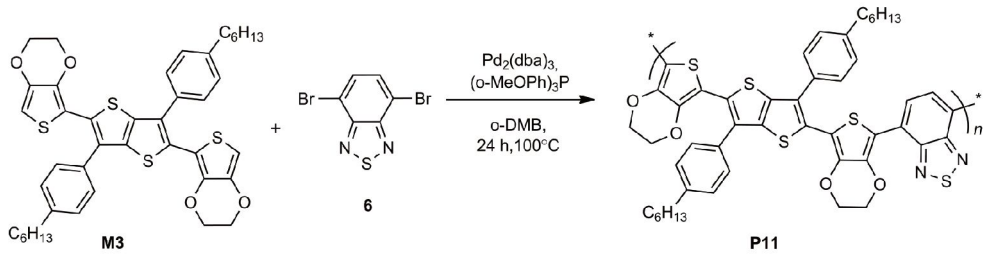

Scheme 4 Palladium catalyzed copolymerization of monomers **M3** and **6** to polymer **P11**.

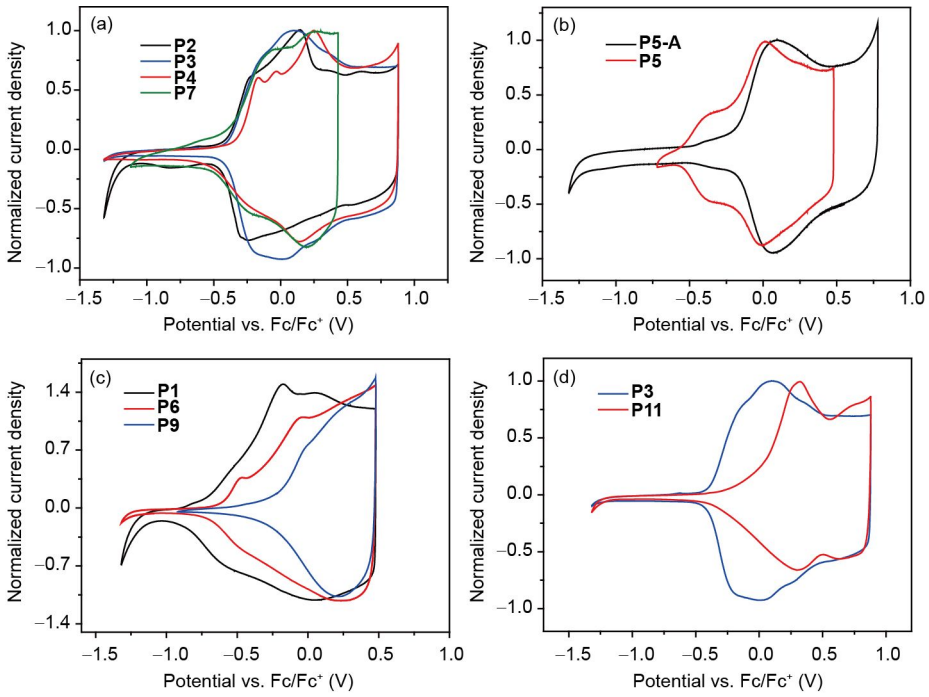

Figure 5 Cyclic voltammograms of polymers **P1**–**P7**, **P9** electrodeposited on Pt disk electrode, and of spray-casted **P11** film in 0.1 M $TBAPF_6$/ACN at a scan rate 100 mV s^{-1} (color online).

through the short S··· O contacts) occurs at the most negative potentials in the series (–0.78 V vs. Fc/Fc^+), which is even more negative than for "unsubstituted" EDOT-TT-EDOT polymer **P6** (–0.64 V) (Table 2). Aryl substituents at positions 3,6- (**P2**–**P4**, **P7**) [43] decrease the HOMO energy level of polymers (an increase of p-doping potentials), but it seems that the main contribution to this behavior is partially breaking the planarity of the main polymer chain by bulky groups, whereas their electronic effects are less pronounced (cf. **P2**–**P4** with **P7** in Figure 5 and Table 2). Yet, electronic effects can not be completely neglected, as an introduction of electron accepting CN group into the phenyl ring gives the polymer which is p-doped at 0.09 V potential higher (–0.36 and –0.45 V for **P7** and **P2**, respectively). Also, electron-donating EDOT groups at the positions 3,6- in the polymer **P5** shift its p-doping potential cathodically to –0.53 V. Nevertheless, in spite of observable electronic effect of the side 3,6-substituents in EDOT-TT-EDOT polymers is clearly seen from these examples, the behavior of pyridine-substituted polymer **P8** is not fully understood. It shows drastic anodic shift of its p-doping process by 0.94 V compared to "unsubstituted" polymer **P6** (from –0.64 V to +0.30 V), and by 0.66 V compared to the polymer **P7** with another electron-accepting 3,6-substituents (4-cyanophenyl). We can speculate that this might be due to the presence of basic nitrogen atom in pyridine, which might effect on the doping/dedoping process of the polymer by partial protonation of the pyridine ring or affecting the proton-transfer processes on electropolymerization process (which might have an influence on the molecular weight and/or the packing fashion of the polymer).

The importance of the mode of an attachment of the EDOT to the TT core becomes obvious when comparing the polymers **P6** and **P9**. More flat, with better degree of conjugation polymer **P6** is a better donor, which is p-doped easier by 0.39 V compared to **P9** ($E_{ox,onset}$=−0.64 and –0.25 V, respectively). It is interesting to compare two polymers, which are obtained by electropolymerization of the monomer **M5** having four EDOT groups on both 2,5- and 3,5-sites. Whereas linear

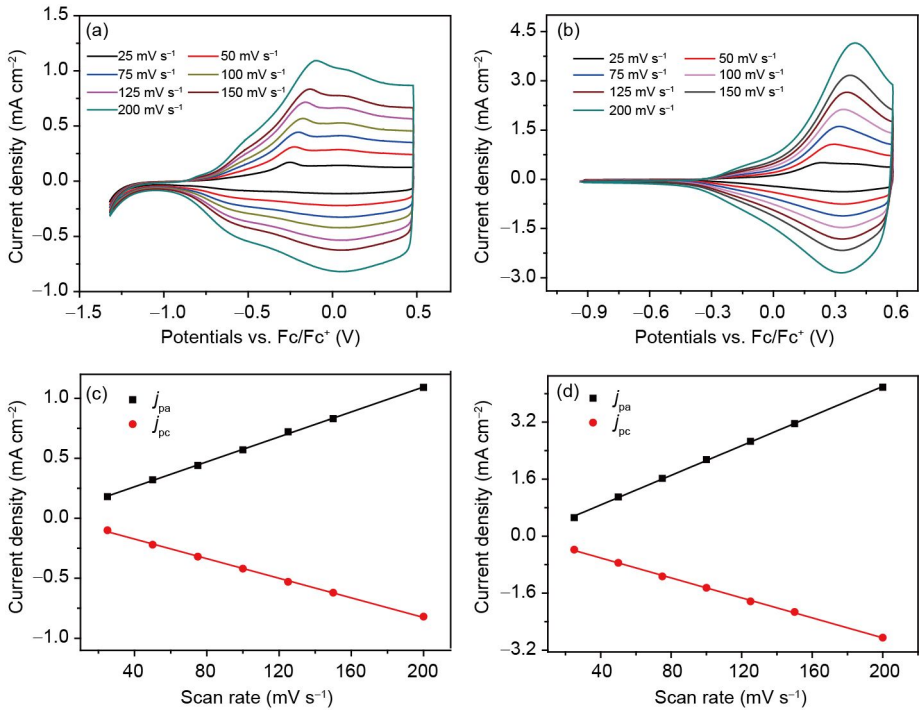

Figure 6 Cyclic voltammograms of (a) **P1** and (b) **P11** polymer films on Pt electrode in monomer-free solution 0.1 M $TBAPF_6$/ACN at different scan rates from 25 to 200 mV s^{-1}. A linear plots of anodic (j_{pa}) and cathodic (j_{pc}) peak current densities versus scan rates for polymers **P1** (c) and **P11** (d), derived from graphs (a) and (b), respectively (color online).

polymer **P5** shows rather low potential of its p-doping (–0.53 V), cross-linked polymer demonstrates substantial anodic shift of its oxidation to –0.26 V.

Obviously, such a cross-linking substantially disturb the planarity of the polymer chain not only due to the increased sterics along the 2,5-(EDOT-TT-EDOT) backbone, but also because the polymerization can occur by coupling at 2,5-/3,6-sites. This decreases the effective conjugation of the polymer **P5-A**, which actually shows the same potential of p-doping as polymer **P9** with 3,6-linkage of the backbone (–0.25 V). Donor-acceptor polymer **P11** shows rather high potential of its p-doping (–0.06 V vs. Fc/Fc^+) compared to other polymers confirming that an introduction of electron-deficient benzothiazole units into the backbone substantially decreases its HOMO energy level over the polymers **P1**–**P7** (although D-A interactions substantially decrease its band gap, as discussed below).

4.3 Spectroelectrochemical properties and colorimetry of the EC polymer films

Spectroelectrochemical (SEC) properties of polymers **P1**–**P9** and **P11**, studied in films deposited on ITO glass are shown in Figure 7 and the data are tabulated in Table 2.

In the neutral form, the absorption maxima of "unsubstituted" polymer P6 and polymer P1 with 3,6- methoxy groups are quite close (569 and 579 nm, respectively), but the onset of the later is strongly red-shifted (by 100 nm) leading to substantial band gap contraction from 1.72 to 1.51 eV. Aryl groups at positions 3,6-[phenyl (**P2**), 4-hexylphenyl (**P3**)] slightly increase the band gap (by 0.06–0.08 eV), but more electron-donating and less bulky thiophenes-functionalized polymers **P4** and **P5** show the band gaps (1.70 and 1.73 eV, respectively) similar to "unsubstituted" polymer **P6** (1.72 eV). In contrast to the oxidation potentials (HOMO) of the polymers, which are substantially different for linear polymer **P5** and cross-linked polymer **P5-A** (by 0.29 eV), the optical band gaps of both polymers in their neutral forms are quite close (1.73 and 1.78 eV, respectively). On the other hand, the change in the mode of an attachment of EDOT units to the TT core (from 3,6- in **P6** to 2,5- in **P9**) results in substantial increase of the band gap (**P9**: 1.92 eV). In the case of polymer **P7** with electron-withdrawing 4-cyanophenyl substituents, substantial band gap contraction is observed (by 0.27 eV compared to **P2**, to 1.53 eV). The same trend is observed in the case of electron deficient pyridine groups (polymer **P8**, 1.66 eV). From analysis of their HOMO/LUMO energies, it is obvious that such a band gap contraction arises from the stronger effect of electron-withdrawing substituents on LUMO than on HOMO (Table 2). As expected, pronounced band gap contraction is also observed for donor-acceptor polymer **P11**, which shows the narrowest band gap in the series (1.46 eV).

An oxidation (p-doping) of all polymers in spectroelectrochemical experiments leads to disappearance of their main π-π* transition band(s) in the visible region on the cost of

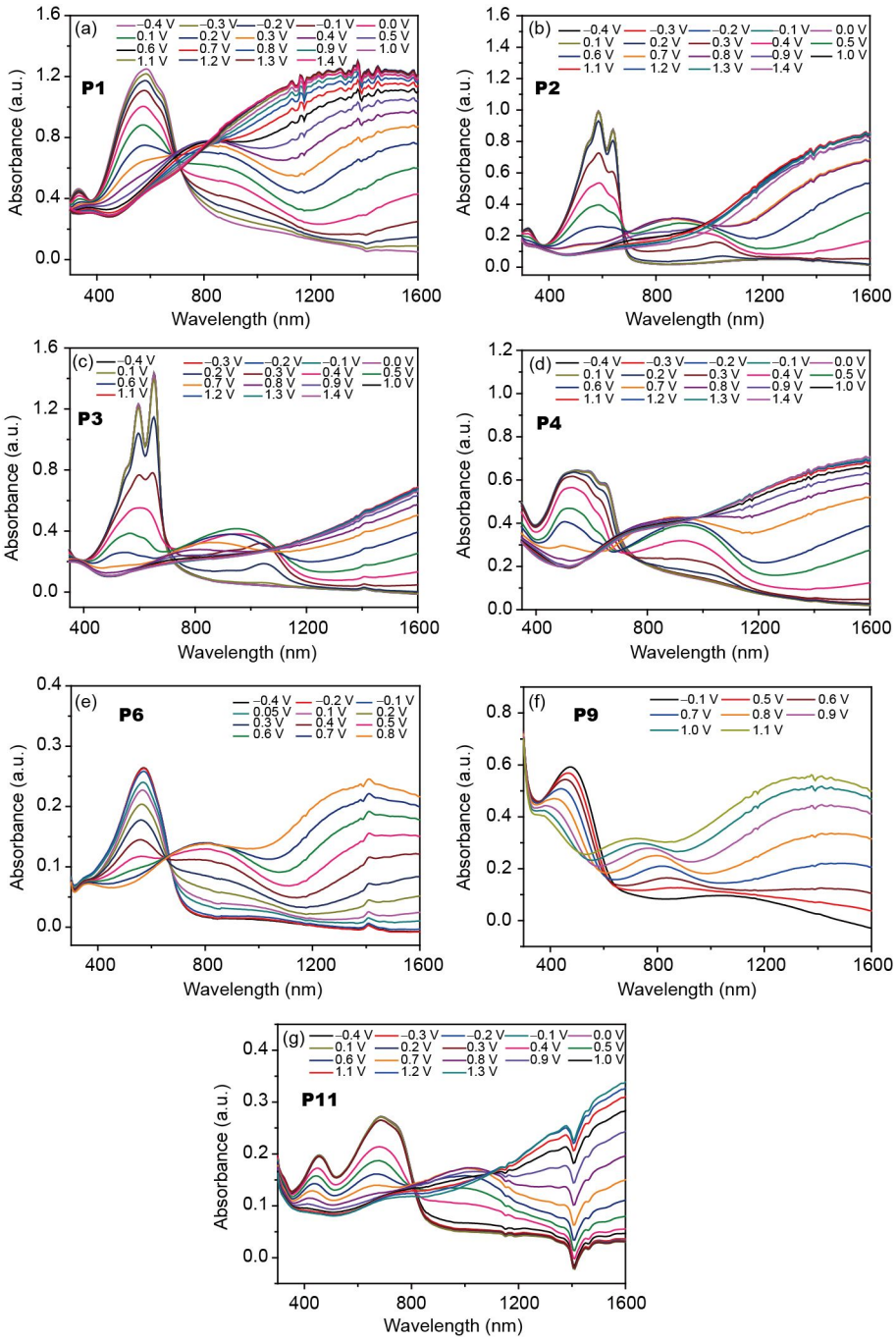

Figure 7 *In-situ* absorption spectra of **P1**–**P4** [43], **P6** [44], **P9** [44] and **P11** polymer films on ITO-glass in monomer-free solution 0.1 M $TBAPF_6$/ACN at different potentials. Applied potentials are versus Ag wire (color online).

growing lower energy, broad absorbtion bands in the long wavelength visible and near infrared (NIR) region attributed to the optical transitions in their polaron and bipolaron states (Figure 7). Oxidized states of the polymers are characterized by two type of optical transitions: (1) broad band (~500–1200 nm) centered around 800–900 nm (it is somewhat blue shifted for **P9** and red-shifted in **P11**) due to polaron carriers; (2) very broad NIR band centered at ~1400 nm (**P1**, **P6**, **P9**) or >1600 nm that belongs to the transitions in bipolarons (Figure 7). Blue tail of these bands in an oxidized state of the polymer is expanded to the visible region dictating (together with short wavelength absorptions) the color of EC polymer on oxidation.

The energy levels diagram and the color palette of the electrochromic EDOT-TT-EDOT polymers in their doped/dedoped states are shown in Figure 8, and the Table 3 summarizes their international commission on illumination (CIE) color coordinates. Aryl-substituted polymers **P2**–**P5** with

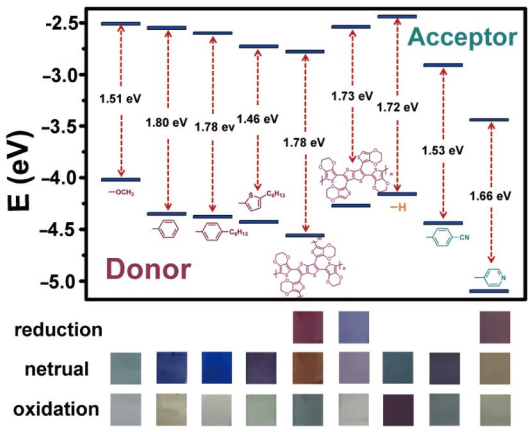

Figure 8 Frontier orbital energy levels and photographs of polymers **P1**–**P8** (films on ITO glass slides) based on EDOT-TT-EDOT core (color online).

electron donating side aryl groups are cathodically coloring polymers: being blue/purple in the neutral state, they undergo bleaching on oxidation to light grey (or pale brownish-/greenish- grey) colors. In contrast, polymers **P7** and **P8** with electron withdrawing 3,6-substituents (4-cyanophenyl, 4-pyridyl) give highly colored films of different colors in both the reduced and the oxidized states. **P7** changes the color from purple (L*=35.7, a*=4.4, b*=−2.5) in the neutral state to a pale grey-blue hue (L*=44.1, a*=−2.4, b*=4.1) in the oxidized state and **P8** shows purple-red color (L*=44.4, a*=7.4, b*=3.1) in fully dedoped state, brown (L=29.6, a*=1.5, b*=−1.4) in the neutral state, and pale grey-green (L*=48.4, a*=3.1, b*=8.9) in the oxidized state. Color values of **P6**, **P7**, **P8** in the neutral state have a trend to a lower L* and to a higher b*, that is to less blue and more yellow hue. In the oxidized states, the color values progress to a lower L* and lower a* that implies to have less purple and more green hue.

It is interesting to compare two polymers, **P5** and **P5-A**, based on tetra(EDOT)-TT monomer **M5**. Linear **P5** polymer (formed on electropolymerization of **M5** at low potential of ~1.0 V) exhibits blue (L*=73, a*=−1.3, b*=−4.5), purple and light blue colors at different applied potentials in SEC. When higher potential (~1.2 V) is applied, the polymer **P5-A** with different EC behavior is formed. **P5-A** changes its color gradually from pinkish-red (L*=63.8, a*=9.1, b*=11.3), to brown and then to light gray [42].

4.4 Contrast and the response time

Optical contrasts, switching times, coloration efficiencies and stability are the important parameters for applications of electrochromic materials. The percent transmittance provides an intuitive assessment of the switching ability of electrochromic materials [17]. At the same time, switching time between the two extreme states (neutral and oxidized/reduced states) is a crucial parameter for some EC applications (e.g. in displays) [39,55].

The "unsubstituted" polymer **P6** shows very high contrast of 79% in the visible region (Table 4). This value slightly decreases on introduction of bulky 3,6-phenyl substitutients (**P2**, 71%) and further decreases on an increase of electron donor ability of aryl groups **P2>P3>P4≈P5** down to 35%–38%. This indicates relatively small effect of the sterics in positions 3,6-, with more important contribution from electronic effects of the side groups to the contrast of this class of EC materials. The above conclusion is also confirmed by low contrast for sterically not crowded polymer with strong electron donating methoxy groups (**P1**, 35%, Table 4 and Figure 9). Interestingly, those electron withdrawing substituents also decrease the contrast even stronger than donor groups (cf.: 24% for **P7** with 4-cyanophenyl- and 17% for **P8** with 4-pyridyl groups). Of course, there is an uncertainty in such a comparison of different polymers associated with measuring the contrasts at different wavelengths, but large changes in the contrasts and analysis of SEC spectra in Figure 7 confirm the validity of such a trend by the electronic effects. Obviously, these differences are, at large extent, due to the different positions (and intensities)

Table 3 CIE 1976 color coordinates of thieno[3,2-*b*]thiophene-based polymers **P1**–**P9**, **P5-A** and **P11**

Polymer	3,6-subst.	2,5-subst.	CIE 1976 (L*; a*; b*)	
			Neutral state	Oxidized state
P1	MeO	EDOT	54.3; 1.8; 1.1	33.9; –1.9; –9.3
P2 [43]	Ph	EDOT	30.5; 3.9; –8.9	33.9; –4.0; –13.5
P3 [43]	HexPh	EDOT	25.7; 2.8; –11.7	35.0; –5.1; –15.5
P4 [43]	HexTh	EDOT	24.8; 1.9; –6.5	33.0; –3.5; –6.2
P5	EDOT	EDOT	54.1; 2.3; –11.8	63.8; –0.2; –1.6
P5-A	EDOT	EDOT	55.9; 9.7; 11.4	56.7; –2.6; 5.5
P6 [44]	H	EDOT	56.5; 1.1; –10.5	50.3; –1.7; 10.7
P7	CNPh	EDOT	35.7; 4.4; –2.5	44.1; –2.4 ; 4.1
P8	Py	EDOT	29.6; 1.5; –1.4	48.4; 3.1; 8.9
P9 [43]	EDOT	H	27.5; –71.1; 1.7	26.8; 30.9; 31.8
P11	–	–	54.7; –2.7; –1.0	60.9; –1.7; –1.9

Table 4 Comparison of contrast (in the visible and NIR region), response time and stability of the polymer films of **P1**–**P9**, **P5-A** and **P11** in 0.1 M $TBAPF_6$/ACN

Polymer	3,6-subst.	2,5-subst.	Contrast, ΔT (%)		Response time (s)		Stability after 100 cycles (switching potentials)
			in Vis (λ)	in NIR (1500 nm)	Oxidation	Reduction	
P1	MeO	EDOT	35 (580 nm)	81	1.85	1.53	66% (–0.8/–1.0 V)
P2	Ph	EDOT	71 (590 nm)	60	1.80	1.10	67% (–0.4/–1.4 V)
P3	HexPh	EDOT	61 (650 nm)	58	2.70	2.00	85% (–0.8/–1.4 V)
P4	HexTh	EDOT	35 (600 nm)	62	1.63	0.96	84% (–0.8/–1.4 V)
P5	EDOT	EDOT	38 (500 nm)	64	0.84	0.85	91% (80%) [42] a) (–0.2/–1.0 V)
P5-A	EDOT	EDOT	22 (500 nm)	75	0.80	0.88	93% (–0.4/–1.3 V)
P6	H	EDOT	79 (570 nm)	48	0.57	1.41	80% (–0.8/–1.0 V)
P7	CNPh	EDOT	24 (570 nm)	62	1.50	2.00	96% (91%) a) (–0.5/–1.0 V)
P8	Py	EDOT	17 (540 nm)	50	2.10	4.10	68% (0/–1.2 V)
P9	EDOT	H	73 (470 nm)	72	1.72	0.83	88% (–0.3/–0.9 V)
P11	–	–	28 (450 nm), 31 (685 nm)	67	0.94	0.91	77% (–0.4/–1.1 V)

a) Values in brackets are after 2000 cycles.

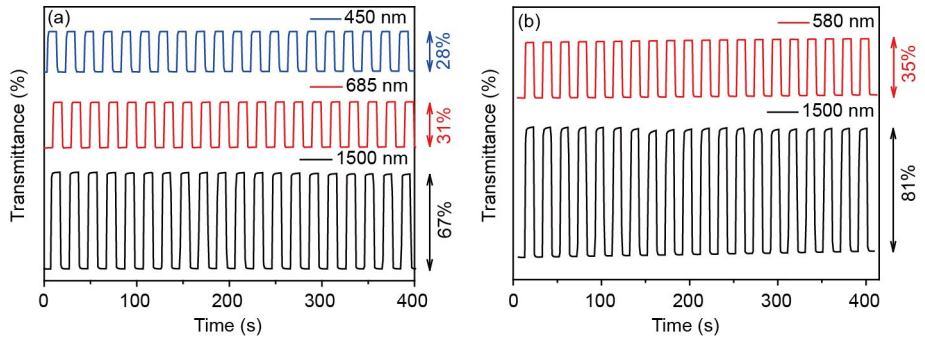

Figure 9 Transmittance-time profile of (a) **P11**, switching between –0.2 and +1.0 V (monitored at 450, 685 and 1500 nm) and (b) **P1**, switching between –0.6 V and +1.0 V (monitored at 580 and 1500 nm) onto ITO coated glass slides in 0.1 M $TBAPF_6$/ACN solution; potential switching time 10 s (color online).

of their polaronic NIR bands, which are expanded to the visible region by their blue tail (Figure 7). With this respect, in design of EC polymers with high contrast it is important to consider not only the structural effects on the absorption of the neutral forms of the polymers but also how the structures affect the transitions in the polaronic states and which factors are important for shifting this polaronic transition down to the NIR region.

It is interesting that the change of the location of EDOT units (2,5- in **P6** vs. 3,6- in **P9**) does not lead to substantial changes in the optical contrast of the polymers switching, as it has on the HOMO energies and the band gaps of the polymers, and **P9** demonstrates rather high contrast of 73%.

Donor-acceptor polymer **P11** also shows relatively low/moderate contrast measured at its two absorption maxima in the visible region (Table 4 and Figure 9).

It is also worth noting that the coloration efficiency of **P5** (234.6 cm^2 C^{-1}) is higher than that of the reported benchmark electrochromic polymer PEDOT (183 cm^2 C^{-1}) [56], and much higher than many inorganic EC materials [57,58]. The switching times of EDOT-TT-EDOT based polymers **P1**–**P9**, **P11** lie in the range of 0.57–2.70 s for oxidation and 0.83–4.10 s for reduction processes and there is no obvious correlation between the structures and their switching times. Nevertheless, some conclusions can be made from analysis of the data in Table 4. "Unsubstituted" parent polymer **P6** shows the lowest response time on oxidation (0.57 s), whereas its back switching is ~3 times longer. Its isomer **P9**, on the contrary, shows twice slower response in the oxidation compared to the reduction process (1.72 and 0.83 s, respectively). Linear and cross-linked polymers **P5** and **P5-A** from tetra-EDOT substituted TT monomer (**M5**) both show rapid switching times of 0.80–0.88 s, with very similar times for oxidation and reduction processes.

4.5 Films morphology and stability

It was demonstrated that the film morphology might strongly affect the EC behavior of the polymers and the performance of the devices [59,60]. Although the mechanism is not fully understood, it is believed that the porous structures should favor the faster switching rate of EC polymers [61,62]. Moreover, in the case of EC polymer films prepared by electropolymerization method, the condition of film growing is important for resulting film morphology. Figure 10 shows images of some representative EDOT-TT-EDOT polymers. All the films obtained by electropolymerization method display typical rough, small grains and spots. Not sterically crowded

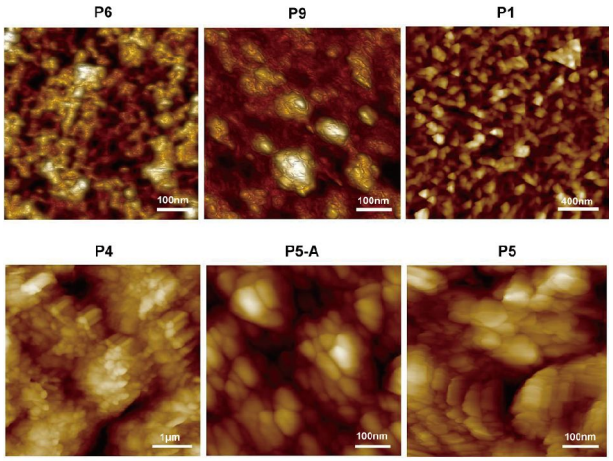

Figure 10 AFM images of polymer films of **P1**, **P4**–**P6**, **P5-A** and **P9** on ITO coated glass slides [42–44] (color online).

polymer **P6** forms compact films with the smooth surface (root-mean-square (RMS) roughness 3.27 nm), while its 3,6-isomer **P9** shows less compact morphology (RMS=7.93 nm) [44]. An increased roughness is observed for 3,6-substituted 2,5-(EDOT-TT-EDOT) polymers. Even **P1** polymer with small methoxy groups shows RMS=30.7 nm. For 3,6-aryl substituted polymers, **P2** shows quite homogeneous flat morphology with RMS=10.5 nm (not shown), but an introduction of long side hexyl chains, as in **P3** (RMS=31.1 nm) and especially in thiophene-substituted analog **P4** (Figure 10, RMS=61.7 nm), gives an aggregated morphology with an increased roughness [43], favorable for doping/dedoping process. Comparison of atomic force microscope (AFM) images for cross-linked **(P5-A)** and linear (**P5**) polymers show that they both have a tendency of aggregation with comparable roughness of the surface, although the shape of the aggregates is different: spherical particles for cross-linked **P5-A** and layered structure in the case of linear **P5** (Figure 10) [42].

The long-time stability upon cycling is a key issue for many commercial applications of EC materials such as e-paper, displays or smart windows. Cyclic voltammetry responses for two polymers, **P1** and **P11**, for the 1st and 100th cycles are shown in Figure 11 and the full data on a decrease of the electroactivity of studied polymers are given in the Table 4. Polymer **P7** shows excellent stability, best in the series, retaining 96% of its electroactivity after 100 cycles (91% after 2000 cycles) (in non-deoxygenated conditions, on an air). Polymers **P5** and **P5-A** are also highly stable on CV cycling (91% and 93%, respectively, after 100 cycles), with no evidence of the cross-linking effects on the cycling stability. Earlier it was shown that oligooxyethylene-bridged cross-linked EDOT-based polymers show remarkable stability (94% electroactivity after 12000 cycles) [63]. Apparently, polymer **P1** with donor methoxy groups shows lower stability (66%), similar to that for phenyl- and 4-pyridyl-substituted polymers **P2** and **P8**. Yet, an introduction of long alkyl chains (in the phenyl and thienyl rings, polymers **P3** and **P4**) improves the stability of the materials on cycling. The nature of the decrease of electroactivity of these polymers requires additional studies. It is not obligatory (and not likely) associated with the polymers degradation, but can be due to other factors including changing the morphology and/or the charge capacity due to mass transfer (penetration or ejection of ions and solvent on cycling). Thus, Huang *et al.* [62] have studied charge trapping in films of various poly(3,4-alkylenedioxythiophenes) on their EC performance and showed that long-term EC stability of polymers on electrochemical cycling/switching is strongly dependent on the number of trapped ions.

5 Conclusions and perspective

In summary, conjugated polymers based on EDOT-TT-EDOT motif (TT=thieno[3,2-*b*]thiophene, EDOT=3,4-ethylenedioxythiophene) represent a promising class of EC materials with broad spectrum of electrochromic behavior, properties of which can be finely tuned by structural variations in the polymer side chain, in the backbone and by changing the fashion of the linkage of the monomer units in the polymers via 2,5- or 3,6- sites of the TT core. The polymers linked at 2,5-sites show lower band gap and higher

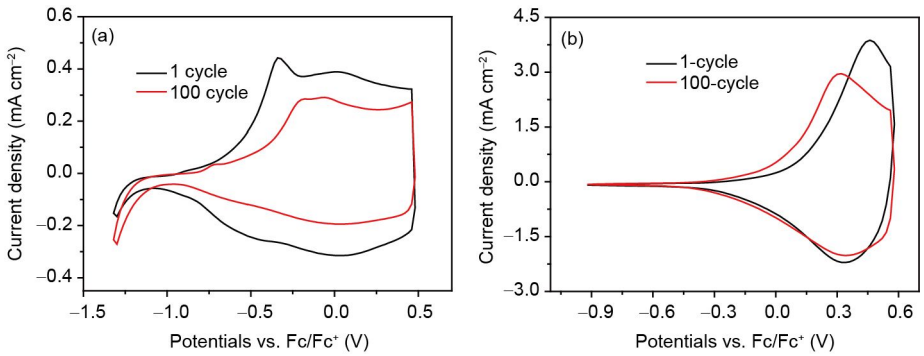

Figure 11 Stability of electrochemical doping/dedoping of (a) **P1** and (b) **P11** polymer films on Pt electrode in 0.1 M $TBAPF_6$/ACN solution at a scan rate of 100 mV s^{-1} on an air (color online).

lying HOMO compared to their 3,6-counterparts. For polymers with 2,5-linage (**P1**–**P8**), substitution at 3,6- positions with electron-donating or electron-withdrawing groups disturb the main chain of the polymer decreasing the HOMO energy levels of the polymers and affecting the polymers band gaps. Both steric and electronic factors contribute to these changes, while sterics seems to be more important contributor. The monomer with four attached EDOT groups to the TT core (**M5**) can be polymerized at 2,5- sites or at both 2,5- and 3,6- sites resulting in linear or crosslinked polymers **P5** and **P5-A**, comparative analysis of which have been presented. Depending on the structure of the building blocks and fashion of polymerization, the polymers offer diverse colors developed in spectroelectrochemical experiments on studies of their electrochromism, such as violet, deep blue, light blue, green, brown, purple-red, pinkish-red, orange-red, light gray, cyan and colorless transparent. These EC polymers show low oxidation potentials, high optical contrast (up to 79% in visible region), short switching time (down to 0.57–0.80 s) and good stability on electrochemical doping/dedoping (up to 96%/100 cycles, 91%/2000 cycles). The polymer **P5** demonstrates very high coloration efficiency (234.6 cm^2 C^{-1}).

Considering the large diversity of possible structural variations in such polymers and wide range of possibilities for combinations of EDOT-TT-EDOT moieties with other conjugated building blocks (one example of such donor-acceptor polymer **P11** has been presented and discussed), we expect an increased interest to this family of EC materials in the nearest future and with further progress in developing novel EC materials based on these promising structures.

Acknowledgments This work was supported by Shenzhen Key Laboratory of Organic Optoelectromagnetic Functional Materials of Shenzhen Science and Technology Plan (ZDSYS20140509094114164), the Shenzhen Peacock Program (KQTD2014062714543296), Shenzhen Science and Technology Research Grant (JCYJ20140509093817690), Nanshan Innovation Agency Grant (KC2015ZDYF0016A), Guangdong Key Research Project (2014B090914003, 2015B090914002), Guangdong Talents Project, the National Basic Research Program of China (2015CB856505), the National Natural Science Foundation of China (51373075), Guangdong Academician Workstation (2013B090400016), the Natural Science Foundation of Guangdong Province (2014A030313800). Igor F. Perepichka thanks to the Santander Universities Research Mobility Award to support his travel to Shenzhen.

Conflict of interest The authors declare that they have no conflict of interest.

1 Dyer AL, Österholm AM, Shen DE, Johnson KE, Reynolds JR. Conjugated electrochromic polymers: structure-driven colour and processing control. In: Mortimer RJ, Rosseinsky DR, Monk PMS, Eds. *Electrochromic Materials and Devices. Part I ElectrochromicMaterials and Processing*. Weinheim: Wiley-VCH, 2015. 113–169
2 Platt JR. *J Chem Phys*, 1961, 34: 862–863
3 Mortimer RJ. *Chem Soc Rev*, 1997, 26: 147
4 Yeh MH, Lin L, Yang PK, Wang ZL. *ACS Nano*, 2015, 9: 4757–4765
5 Runnerstrom EL, Llordés A, Lounis SD, Milliron DJ. *Chem Commun*, 2014, 50: 10555–10572
6 Granqvist CG, Azens A, Isidorsson J, Kharrazi M, Kullman L, Lindström T, Niklasson GA, Ribbing CG, Rönnow D, Strømme Mattsson M, Veszelei M. *J Non-Crystalline Solids*, 1997, 218: 273–279
7 Österholm AM, Shen DE, Kerszulis JA, Bulloch RH, Kuepfert M, Dyer AL, Reynolds JR. *ACS Appl Mater Interfaces*, 2015, 7: 1413–1421
8 Beaujuge PM, Reynolds JR. *Chem Rev*, 2010, 110: 268–320
9 Xu T, Walter EC, Agrawal A, Bohn C, Velmurugan J, Zhu W, Lezec HJ, Talin AA. *Nat Commun*, 2016, 7: 10479
10 Sonmez G, Sonmez HB. *J Mater Chem*, 2006, 16: 2473–2477
11 Invernale MA, Ding Y, Sotzing GA. *ACS Appl Mater Interfaces*, 2010, 2: 296–300
12 Yu H, Shao S, Yan L, Meng H, He Y, Yao C, Xu P, Zhang X, Hu W, Huang W. *J Mater Chem C*, 2016, 4: 2269–2273
13 Chandrasekhar P, Zay BJ, Birur GC, Rawal S, Pierson EA, Kauder L, Swanson T. *Adv Funct Mater*, 2002, 12: 95–103
14 Chandrasekhar P, Zay BJ, McQueeney T, Scara A, Ross D, Birur GC, Haapanen S, Kauder L, Swanson T, Douglas D. *Synth Met*, 2003, 135-136: 23–24
15 Abidin T, Zhang Q, Wang KL, Liaw DJ. *Polymer*, 2014, 55: 5293–5304
16 Beverina L, Pagani GA, Sassi M. *Chem Commun*, 2014, 50: 5413–5430
17 Amb CM, Dyer AL, Reynolds JR. *Chem Mater*, 2011, 23: 397–415
18 Bulloch RH, Kerszulis JA, Dyer AL, Reynolds JR. *ACS Appl Mater Interfaces*, 2015, 7: 1406–1412
19 Kerszulis JA, Amb CM, Dyer AL, Reynolds JR. *Macromolecules*, 2014, 47: 5462–5469
20 Bulloch RH, Reynolds JR. *J Mater Chem C*, 2016, 4: 603–610
21 Kirchmeyer S, Reuter K. *J Mater Chem*, 2005, 15: 2077–2088
22 Jonas F, Schrader L. *Synth Met*, 1991, 41: 831–836
23 Heywang G, Jonas F. *Adv Mater*, 1992, 4: 116–118
24 Dietrich M, Heinze J, Heywang G, Jonas F. *J Electroanal Chem*, 1994, 369: 87–92
25 Xia Y, Ouyang J. *ACS Appl Mater Interfaces*, 2012, 4: 4131–4140
26 Kim YH, Sachse C, Machala ML, May C, Müller-Meskamp L, Leo K. *Adv Funct Mater*, 2011, 21: 1076–1081
27 Heuer HW, Wehrmann R, Kirchmeyer S. *Adv Funct Mater*, 2002, 12: 89–94
28 Invernale MA, Bokria JG, Ombaba M, Lee KR, Mamangun DMD, Sotzing GA. *Polymer*, 2010, 51: 378–382
29 Groenendaal L, Zotti G, Aubert PH, Waybright SM, Reynolds JR. *Adv Mater*, 2003, 15: 855–879
30 Groenendaal L, Jonas F, Freitag D, Pielartzik H, Reynolds JR. *Adv Mater*, 2000, 12: 481–494
31 Roncali J, Blanchard P, Frère P. *J Mater Chem*, 2005, 15: 1589–1610
32 Beaujuge PM, Amb CM, Reynolds JR. *Acc Chem Res*, 2010, 43: 1396–1407
33 Cinar ME, Ozturk T. *Chem Rev*, 2015, 115: 3036–3140
34 Skabara PJ. Fused oligothiophenes. In: Perepichka IF, Perepichka DF, Eds. *Handbook of Thiophene-Based Materials: Applications in Organic Electronics and Photonics. Volume 1: Synthesis and Theory*. New York: John Wiley & Sons, 2009. 219–254
35 Zhang Q, Wang Y, Kan B, Wan X, Liu F, Ni W, Feng H, Russell TP, Chen Y. *Chem Commun*, 2015, 51: 15268–15271
36 Tang W, Ke L, Tan L, Lin T, Kietzke T, Chen ZK. *Macromolecules*, 2007, 40: 6164–6171

37 Perepichka IF, Perepichka DF, Meng H, Wudl F. *Adv Mater*, 2005, 17: 2281–2305
38 Hamaguchi A, Negishi T, Kimura Y, Ikeda Y, Takimiya K, Bisri SZ, Iwasa Y, Shiro T. *Adv Mater*, 2015, 27: 6606–6611
39 Toksabay S, Hacioglu SO, Unlu NA, Cirpan A, Toppare L. *Polymer*, 2014, 55: 3093–3099
40 Turbiez M, Frère P, Leriche P, Mercier N, Roncali J. *Chem Commun*, 2005, 1161–1163
41 Capan A, Ozturk T. *Synth Met*, 2014, 188: 100–103
42 Shi J, Zhu X, Xu P, Zhu M, Guo Y, He Y, Hu Z, Murtaza I, Yu H, Yan L, Goto O, Meng H. *Macromol Rapid Commun*, 2016, 37: 1344–1351
43 Xu P, Murtaza I, Shi J, Zhu M, He Y, Yu H, Goto O, Meng H. *Polym Chem*, 2016, 7: 5351–5356
44 Zhu X, Zhu Y, Murtaza I, Shi J, He Y, Xu P, Zhu M, Goto O, Meng H. *RSC Adv*, 2016, 6: 75522–75529
45 Raimundo JM, Blanchard P, Frère P, Mercier N, Ledoux-Rak I, Hierle R, Roncali J. *Tetrahedron Lett*, 2001, 42: 1507–1510
46 Turbiez M, Frère P, Roncali J. *J Org Chem*, 2003, 68: 5357–5360
47 Turbiez M, Frère P, Allain M, Videlot C, Ackermann J, Roncali J. *Chem Eur J*, 2005, 11: 3742–3752
48 Turbiez M, Hergué N, Leriche P, Frère P. *Tetrahedron Lett*, 2009, 50: 7148–7151
49 Us CN, Icli Ozkut M. *Macromolecules*, 2016, 49: 3009–3015
50 Balan A, Baran D, Gunbas G, Durmus A, Ozyurt F, Toppare L. *Chem Commun*, 2009, 6768
51 Amb CM, Beaujuge PM, Reynolds JR. *Adv Mater*, 2010, 22: 724–728
52 Wang JL, Yin QR, Miao JS, Wu Z, Chang ZF, Cao Y, Zhang RB, Wang JY, Wu HB, Cao Y. *Adv Funct Mater*, 2015, 25: 3514–3523
53 Ledwon P, Zassowski P, Jarosz T, Lapkowski M, Wagner P, Cherpak V, Stakhira P. *J Mater Chem C*, 2016, 4: 2219–2227
54 Gu PY, Zhang J, Long G, Wang Z, Zhang Q. *J Mater Chem C*, 2016, 4: 3809–3814
55 Shi P, Amb CM, Dyer AL, Reynolds JR. *ACS Appl Mater Interfaces*, 2012, 4: 6512–6521
56 Gaupp CL, Welsh DM, Rauh RD, Reynolds JR. *Chem Mater*, 2002, 14: 3964–3970
57 Liang L, Zhang J, Zhou Y, Xie J, Zhang X, Guan M, Pan B, Xie Y. *Sci Rep*, 2013, 3: 1936
58 Yao DD, Rani RA, O'Mullane AP, Kalantar-zadeh K, Ou JZ. *J Phys Chem C*, 2014, 118: 10867–10873
59 Ye Q, Neo WT, Lin T, Song J, Yan H, Zhou H, Shah KW, Chua SJ, Xu J. *Polym Chem*, 2015, 6: 1487–1494
60 Neo WT, Ye Q, Lin TT, Chua SJ, Xu J. *Sol Energ Mat Sol C*, 2015, 136: 92–99
61 Tehrani P, Hennerdal LO, Dyer AL, Reynolds JR, Berggren M. *J Mater Chem*, 2009, 19: 1799–1802
62 Huang JH, Hsu CY, Hu CW, Chu CW, Ho KC. *ACS Appl Mater Interfaces*, 2010, 2: 351–359
63 Perepichka IF, Besbes M, Levillain E, Sallé M, Roncali J. *Chem Mater*, 2002, 14: 449–457